Available online at www.sciencedirect.com
SCIENCE DIRECT®
Biochimica et Biophysica Acta 1661 (2004) 87–96
BIOCHIMICA ET BIOPHYSICA ACTA
BBA
www.bba-direct.com

Dynamics of pH-dependent self-association and membrane binding of a dicarboxylic porphyrin: a study with small unilamellar vesicles

Stéphanie Bonneau, Nathalie Maman, Daniel Brault*

Laboratoire de Physicochimie Biomoléculaire et Cellulaire, CNRS UMR 7033, Université Pierre et Marie Curie, 75005 Paris, France
Laboratoire de Photobiologie, Muséum National d'Histoire Naturelle, 75005 Paris, France

Received 1 October 2003; received in revised form 3 December 2003; accepted 3 December 2003

Abstract

Steady-state and stopped-flow measurements of the absorbance and fluorescence of aqueous solutions were performed to characterize the pH-dependent ionization and aggregation states of deuteroporphyrin. Porphyrin self-association promoted by neutralization of the carboxylic groups takes place within a few milliseconds impeding characterization of the monomer ionization states. Extrapolation at infinite dilution of the values obtained from steady-state measurements yielded the p*K*s of the carboxylic groups (6.6, 5.3) and inner nitrogens (4.1, 2.3). The kinetics of interactions of the porphyrin with unilamellar fluid state dioleoylphosphatidylcholine vesicles was examined in a large pH range, with focus on the entry step. From alkaline pH to a value of 6.5, the entrance rate is maximal (1.69×10^6 M^{-1} s^{-1} versus phospholipid concentration). It decreases to 2.07×10^5 M^{-1} s^{-1} at lower pH with an apparent p*K* of 5.39. This effect appears to be related to the formation of porphyrin dimer rather than to the protonation of inner nitrogen. In keeping with previous data, these results support the concept of a pH-mediated selectivity of carboxylic porphyrins for tumor. They also indicate that the propensity of these molecules to self-associate at low pH could yield to some retention in acidic intracellular vesicles of the endosome/lysosome compartment.

Keywords: Photosensitizer; Tumor; Membrane model; Passive transport; Kinetic; Stopped-flow

1. Introduction

Porphyrins belong to an important class of photosensitizers [1] used in photodynamic therapy (PDT). This new modality is based on the activation by light of these molecules that are accumulated to some extent in proliferating tissues. A dual selectivity results from the retention of the dye and the possibility to restrict the light irradiation to the diseased area. This approach has been developed for tumor therapy [2–4]] and more recently for the treatment of the age-related macular degeneration [5,6]. A porphyrin-based preparation, Photofrin®, has received the first drug-approval for tumor therapy.

Upon light activation, photosensitizers produce short-lived species, such as radicals and singlet oxygen able to chemically damage various biomolecules. Owing to their reactivity, the diffusion distance of these species does not exceed the size of cellular organelles. Thereby, primary molecular damages affect subcellular structures labeled by the photosensitizer. As a matter of fact, phototoxicity and the mechanism of cell death (apoptosis or necrosis) strongly depend on the subcellular localization of the photosensitizer [7–9].

It has been suggested that the affinity of lipophilic photosensitizers for low-density lipoproteins, LDL [10], might account for their selective retention by tumors [11–13]. Indeed, the number of receptors to LDL is increased in proliferating tissues [14,15]. However, we recently showed that the exchange of a dicarboxylic

* Corresponding author. Laboratoire de Photobiologie, Muséum National d'Histoire Naturelle, 43, Rue Cuvier, 75231 Paris Cedex 05, France. Tel.: +33-1-40-79-36-97; fax: +33-1-40-79-37-16.
E-mail address: brault@mnhn.fr (D. Brault).

0005-2736/$ - see front matter © 2004 Elsevier B.V. All rights reserved.
doi:10.1016/j.bbamem.2003.12.002

porphyrin, deuteroporphyrin, between LDL and the bulk medium is extremely fast [16]. Then, contribution of passive diffusion through the plasmic membrane must be considered. Also, diffusion through internal membranes is likely to be the main route for photosensitizer redistribution inside cells. The diffusion of uncharged molecules through membranes is generally correlated with their water/oil partition coefficient [17]. For amphiphilic porphyrins, the use and limitation of lipophilicity parameters for the prediction of membrane binding have been discussed [18].

The increase of anaerobic metabolism of glucose in hyper-proliferating tissues leads to lactic acid excretion. In poorly drained tumor tissues, the consequence is an acidification of the extracellular medium by about 0.5 pH unit [19]. As the lipophilicity of some photosensitizers such as Photofrin® is increased at lower pH through the neutralization of carboxylic chains, this property has been suggested to contribute to the retention of these molecules by tumors [20–22]. This hypothesis is supported by studies on animals [23], cells [24] and on the interactions of dicarboxylic porphyrins with membrane models [20,25]. It must be pointed out that important pH gradients also exist within cells. The internal pH of lysosomes is around 5. Even if photosensitizers are incorporated by endocytosis, pH effects may come into play.

It follows that the knowledge of factors governing the dynamics of diffusion of photosensitizers across membranes within a large range of pH values is important. We addressed this question in a series of studies on deuteroporphyrin, a dicarboxylic porphyrin that can be considered as the archetype of Photofrin® components. Small unilamellar vesicles were used to simulate membranes. A method based on the transfer of the porphyrin from vesicles to albumin allowed us to determine the rate constants for the flip-flop of the molecule between the two hemilayers and for its exit from the membrane [26]. Drastic effects of pH on the rate constants were observed. The permeation of these molecules from a moderately acid to a neutral aqueous compartment was found to be strongly favored kinetically [27,28].

However, little data were available on the rate on entry of the porphyrin into the bilayer as a function of pH. In fact, such measurements are difficult due to the poor stability of aqueous solutions of deuteroporphyrin between pH 6 and 3. The porphyrin self-associates in this pH range ultimately leading to precipitate formation [29]. This behavior is linked to protonation equilibrium of propionic chains and imino nitrogens of the porphyrin. As a consequence, the p*K* values of these groups are subjected to large uncertainty. In the present work, we used fluorimetric titration and stopped-flow measurements in order to reexamine these p*K* values with regard to the self-association problem. Then, our purpose was to correlate the ionization state of the porphyrin in the bulk aqueous medium with its rate of association to the outer hemilayer of the membrane.

2. Materials and methods

2.1. Materials

Deuteroporphyrin, the structure of which is shown in Fig. 1, was prepared as described previously [20]. Its purity was determined to be better than 99% by HPLC. Stock solutions were prepared in distilled tetrahydrofuran (THF) and kept at − 18 °C. Diluted experimental solutions were used without delay and renewed frequently. This procedure was found to minimize aggregation and adsorption of DP on glass. The porphyrin solutions were handled in the dark to avoid any photobleaching.

2.2. Vesicles preparation

Small unilamellar vesicles were made from dioleoylphosphatidylcholine (C18:1) obtained from Avanti Polar Lipids (Alabaster, AL) as chloroformic solutions. After evaporation of chloroform, lipids were dispersed in 0.15 M NaCl solutions buffered to various pH values with phosphate 20 mM by vortexing. The liposome suspension was extruded 8–10 times through a stack of two polycarbonate membrane

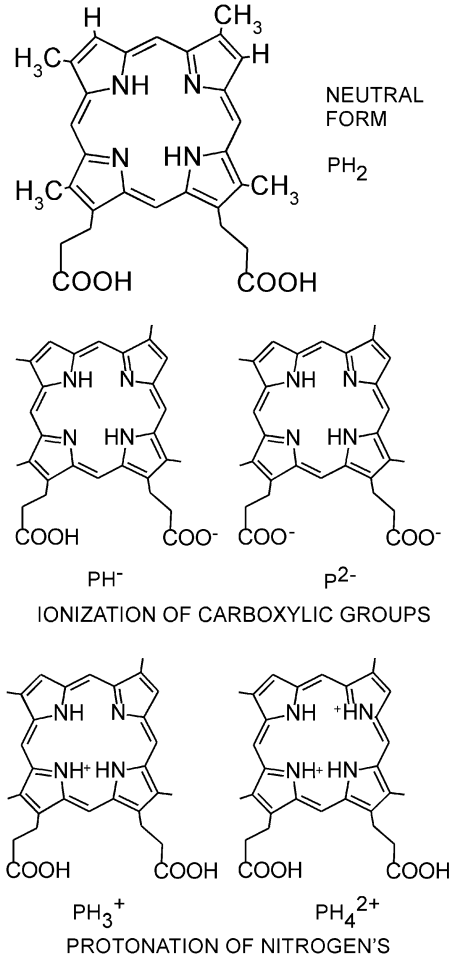

Fig. 1. Structure and ionization states of deuteroporphyrin.

filters (Poretics, Livermore, CA) with pores of 50 nm using an extruder device (Lipex Biomembranes, Vancouver, CA) thermostated at 25 °C.

2.3. Measurements

Emission spectra were measured using a SPEX spectrofluorimeter (Edison, NJ). Recording was generally started 2 min after the preparation of the solutions under study.

An Applied Photophysics (Leatherhead, UK) stopped-flow apparatus with mixing time of 1.2 ms was used to record time-resolved spectra and for kinetic measurements. The mixing ratio was 1:1. The light source was a 150-W xenon arc lamp. Absorption spectra were collected in the range 200–750 nm by using a photodiode array with a resolution of 2.17 nm. At the maximum scan speed, spectra were recorded every 2.56 ms. Then, at the best, the first spectrum can be recorded 3.76 ms after mixing begun. For fast kinetics measurements, the excitation light was passed through a monochromator with slits generally set to give a bandwidth of 4.65 nm. Fluorescence emission was collected above 610 or 590 nm using low-cut filters (Oriel, France). The fluorescence signal was fed to a RISC workstation (Acorn Computers, UK) and analyzed using the software provided by the manufacturer. All the measurements were performed at 25 °C. In a previous report [26], we have determined the affinity constant of deuteroporphyrin for vesicles extruded on 50-nm pores either by using steady-state techniques or stopped-flow experiments. The same value was obtained by these two techniques indicating that the vesicles are not altered during the rapid mixing process.

2.4. Adjustment of porphyrin solution to low pH with pre-mixing stopped-flow accessory

This method was applied to study the association of porphyrins with vesicles in a large range of pH. First, we controlled by absorption spectroscopy that porphyrin solutions at high pH (8.5–9) do not self-associate and are stable. In fact, porphyrin solutions were found to obey Beer's law up to 3×10^{-6} M and were characterized by a well-defined Soret band at 395 nm. Then, the aim was to quickly prepare solutions at the desired acidic pH before self-association could take place. We used the pre-mixing accessory of the stopped-flow apparatus to this purpose. It makes it possible to mix two solutions before a conventional stopped-flow experiment. In the first step, the basic porphyrin solution was mixed with an aqueous solution buffered at acid pH so that the mixture of the two solutions gives the desired final pH. The phosphate molarities of the two solutions were adjusted to obtain a final phosphate concentration of 20 mM. Then, 10 ms later, the resulting solution was mixed with a liposomes suspension at the same pH using the usual mixing chamber. The elapsed time between the two steps was the minimal value available. It was believed to be sufficient to allow completion of the protonation and deprotonation steps involving the porphyrin.

3. Results

3.1. Ionization states of deuteroporphyrin in aqueous solution

Deuteroporphyrin can present different ionization states as shown in Fig. 1. At acid pH, one or two protons can be bound to the inner nitrogen yielding the monocationic and dicationic forms, respectively. Successive deprotonations of the carboxylic groups lead to monoanionic and dianionic forms. The p*K*s of these various groups were determined previously [20]. However, as outlined above, the accuracy of these values might be rather weak. Indeed, neutralization of the carboxylic groups promotes self-association of porphyrins in solution. This process is accompanied by changes in absorption spectra and a strong inhibition of the fluorescence, which might introduce bias in p*K* determination. As a matter of fact, significant differences in p*K* values were found when hematoporphyrin, another dicarboxylic porphyrin, was titrated by using acid or basic solutions [22]. The p*K* values of deuteroporphyrin are reexamined now with regard to the self-association problem.

3.1.1. Time-resolved absorption spectra

At low porphyrin concentration, it can be considered that self-association is restricted to dimer formation [30]. The dimerization constant for deuteroporphyrin in phosphate buffer saline (pH 7.2) was previously determined to be 2.3×10^{6} M^{-1} [31]. In neutral solutions, the monomer and dimer forms can be clearly identified by their near-UV bands positioned at 395 and 370 nm, respectively. First, we tried to distinguish the protonation and self-association processes kinetically. The rationale was as follows. The porphyrin was dissolved in a solution of phosphate buffer 1 mM adjusted to pH 9.5. At this pH, carboxylic chains are ionized preventing self-association in the range of concentration used ($< 3 \times 10^{-6}$ M). This solution was mixed, in the stopped-flow apparatus, with a 39 mM phosphate buffer solution adjusted to acidic pH. This value was determined according to preliminary experiments so that the mixture possesses the desired working pH value. All the solutions contained 0.15 M NaCl. The phosphate concentration after mixing was 20 mM. The use of a higher phosphate concentration for the acidic solution made it possible to reach pH as low as 1.8 after mixing. Two absorption spectra were recorded, 2.56 ms and 1 s after mixing, respectively. The final porphyrin concentration was as weak as possible (5.7×10^{-7} M), in order to minimize dimerization.

Results are reported in Fig. 2. At a final pH of 7.02, the two spectra are identical. They exhibit a peak at 395 nm, characteristic of the monomer form. However, a shoulder around 370 nm indicates a significant contribution of dimer

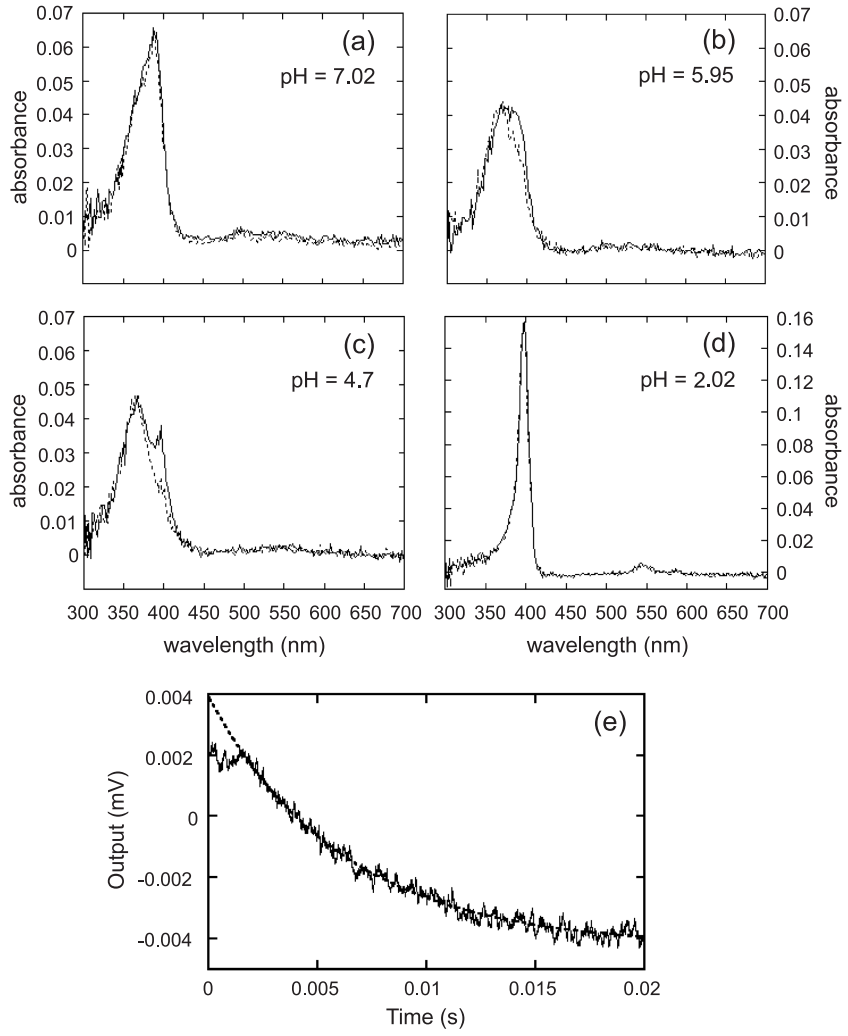

Fig. 2. Time-resolved studies of changes of deuteroporphyrin spectra in aqueous solution induced by pH jump. Top: Absorption spectra of porphyrin solutions (5.7×10^{-7} M) recorded 2.56 ms and 1 s after mixing with acid buffer. The final pH is 7.02 (a), 5.95 (b), 4.7 (c) and 2.02 (d). Bottom: (e) Fluorescence changes following acidification of a deuteroporphyrin solution (5.5×10^{-8} M). The final pH is 5.95 (see text for experimental details).

even at the shortest time. In fact, by using a dimerization constant of 2.3×10^{6} M^{-1} [31], it can be calculated that, at equilibrium, only 46% of the porphyrin remains as monomer at the concentration used. At pH 5.95 and 4.7, although some change can be seen between the two spectra, the dimer is the predominant form even for the initial record. In all cases, the dimerization is too rapid, which does not allow investigation of the protonation steps involving the monomer. At pH 2.02, the spectra are identical with a major peak at 400 nm corresponding to the monomeric dicationic form, as expected [32].

We tried to distinguish the protonation and dimerization steps using fluorescence measurements and the same protocol for mixing. The sensitivity of fluorescence allows the use of lower concentrations, which would limit the rate of dimerization. Also, the fluorescence properties of the porphyrin species are likely to be affected by solvation that depends on protonation states [33]. Fluorescence emission was recorded above 590 nm using a low-cut filter. The excitation wavelength was set at 395 nm. The final porphyrin concentration was 5.5×10^{-8} M. The kinetics recorded over various time scales (20 ms, 200 ms, 1 s) failed to reveal successive processes. They were correctly fitted by monoexponential curves as exemplified in Fig. 2e for an experiment performed at pH 5.95.

3.1.2. Fluorimetric titration at various porphyrin concentrations

Concentration effects on the pK values measured at equilibrium could give some information on the monomer by extrapolation to a null porphyrin concentration [34]. A series of acid–base titration has been performed with various porphyrin concentrations (3.6×10^{-7}, 1.8×10^{-7}, 3.6×10^{-8} and 7.2×10^{-9} M). Fig. 3 displays typical sets of fluorescence emission spectra. Around pH 4.7, the overall fluorescence is weak, which corresponds to the greatest formation of dimers. Lowering the pH to 1.8 leads to the appearance of bands at 592 and 650 nm. On the other hand,

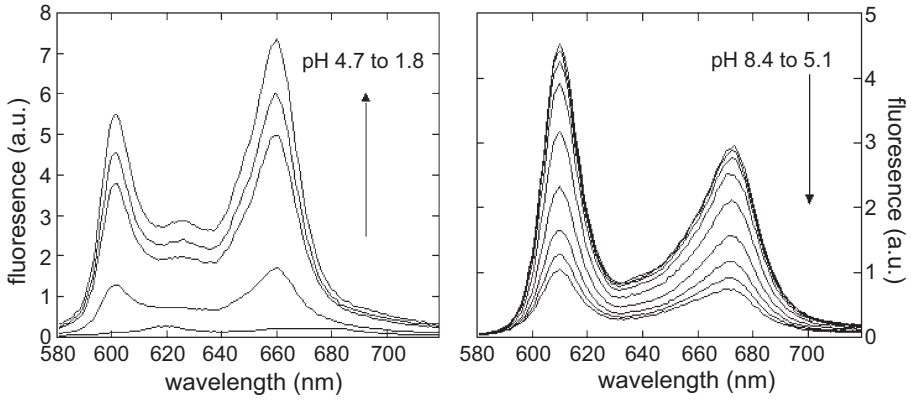

Fig. 3. Fluorimetric titration of deuteroporphyrin (3.6×10^{-7} M) in aqueous solution containing 20 mM phosphate buffer and 0.15 M NaCl. Fluorescence emission spectra selected at various pH in the acidic region (left, pH: 1.8, 2.02, 2.95, 3.6 and 4.7) and slightly acidic to slightly alkaline region (right, 5.1, 5.3, 5.5, 5.7, 6.2, 6.7, 7.02, 7.55 and 8.4).

buildup of fluorescence at 610 and 670 nm is observed when pH is increased. The following equilibriums were postulated:

$$PH_4^{2+} \overset{K_{N2}}{\rightleftharpoons} PH_3^{+} \overset{K_{N1}}{\rightleftharpoons} PH_2 \overset{K_{A1}}{\rightleftharpoons} PH^{-} \overset{K_{A2}}{\rightleftharpoons} P^{2-}$$

On the basis of spectral characteristics and the extent of fluorescence extinction through dimerization, it is postulated that the neutral form, PH_2, is predominant around pH 4.7. Successive formations of the mono- and dicationic forms arise between pH 4.7 and 1.8. The mono- and dianion forms are formed at higher pH. Titration curves in these two pH ranges are given in Fig. 4 for the most significant wavelengths. In keeping with a previous study [20], data were fitted according to the equation:

$$F = \frac{\alpha'}{\alpha} C$$

where C is the total porphyrin concentration and F the total fluorescence intensity at a given pH. For each pH range, the various constants are defined as in the former report [20]:

pH range

$$5 - 8.4 \begin{cases} \alpha = 1 + \dfrac{K_{A1}}{[H^+]} + \dfrac{K_{A1} \cdot K_{A2}}{[H^+]^2} \\ \alpha' = f_{PH2} + f_{PH} \cdot \dfrac{K_{A1}}{[H^+]} + f_P \cdot \dfrac{K_{A1} \cdot K_{A2}}{[H^+]^2} \end{cases} \quad (1)$$

pH range

$$1.8 - 4.7 \begin{cases} \alpha = 1 + \dfrac{[H^+]}{K_{N1}} + \dfrac{[H^+]^2}{K_{N1} \cdot K_{N2}} \\ \alpha' = f_{PH2} + f_{PH3} \cdot \dfrac{[H^+]}{K_{N1}} + f_{PH4} \cdot \dfrac{[H^+]^2}{K_{N1} \cdot K_{N2}} \end{cases} \quad (2)$$

It is assumed that the fluorescence emitted by each form is directly proportional to its concentration via proportionality factors noted f (the charges of the various forms are omitted in these notations).

The values of pKs have been determined for four porphyrin concentrations and plotted in Fig. 5. The results confirm that pK values are biased because of porphyrin dimerization. Extrapolation of the curves to the intercept gives $pK_{A2} = 6.6$, $pK_{A1} = 5.3$, $pK_{N1} = 4.1$ and $pK_{N2} = 2.3$. These values represent better the properties of the monomeric form of the porphyrin.

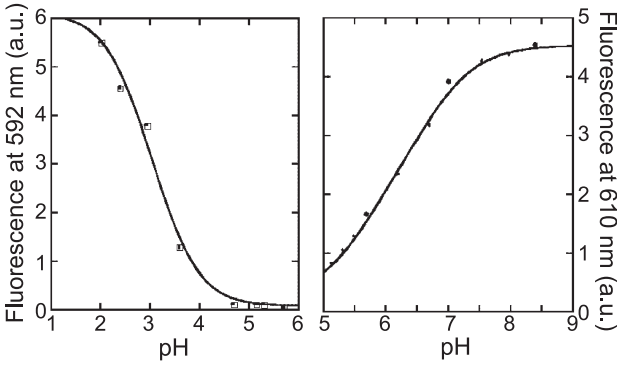

Fig. 4. Titration curves at the most significant wavelengths corresponding to the spectral changes shown in Fig. 3: left, 592 nm; right, 610 nm.

3.2. Incorporation of deuteroporphyrin in lipidic vesicles

3.2.1. Kinetics of association of porphyrin with vesicles at various pH

As previously shown [20,35], the transfer of monomeric deuteroporphyrin from an aqueous environment towards the lipidic phase of vesicles is accompanied by large changes in fluorescence emission spectra that can be easily monitored. It should be noted that the dimers of deuteroporphyrin do not fluoresce.

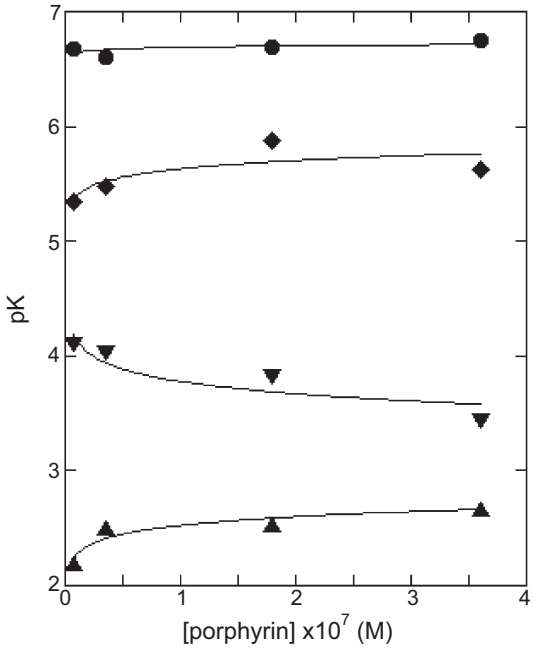

Fig. 5. Effect of concentration on apparent pK values of deuteroporphyrin. The porphyrin concentrations are 3.6×10^{-7}, 1.8×10^{-7}, 3.6×10^{-8}, and 7.2×10^{-9} M.

The association of porphyrins, or any other drug, with vesicles involves two steps. First, the drug enters into the outer leaflet of the bilayer. The second step involves the transfer of the drug through the bilayer that results in equilibrated partition between the two leaflets. Amphiphilic molecules bearing polar chains with asymmetrical distribution such as deuteroporphyrin become localized in the two hemileaflets with their polar moiety oriented towards the aqueous interfaces. In these conditions, the two steps can be distinguished. A theoretical description of these processes has been proposed [26], according to the scheme below, where P_f, P_o and P_i are the concentrations of porphyrin free in the bulk aqueous solution, incorporated into the outer leaflet or the inner one, respectively:

$$P_f + L \underset{k_{off}}{\overset{k_{on}}{\rightleftarrows}} P_o \underset{k_{to}}{\overset{k_{ti}}{\rightleftarrows}} P_i$$

L is the vesicle concentration that will be expressed in terms of phospholipid molecules in the following. In the former and present studies, the phospholipid concentration largely exceeded that of the porphyrin. Hence, the entry into the vesicles obeys pseudo-first order kinetics with a constant $k'_{on}=k_{on}\times[L]$.

Theoretical calculations predict biexponential signals with the rate constants k_1 and k_2:

$$k_1 = k_{on}\times[L] + k_{off} + k_{to} + k_{ti} \quad (3)$$

$$k_2 = k_{to} + k_{ti} \quad (4)$$

The rate of the flip-flop between the two layers (k_{to}, k_{ti}) strongly depends on the bilayer thickness and the ionization state of the side chains. In the present study, we used C18:1 phospholipids. The bilayer thickness was large to insure that the rate of transfer through the membrane was slow enough in all the pH range investigated [28]. Then, the equilibrium involving the entry of the porphyrin within the outer layer of the vesicles can be monitored easily and the rate constants k_{to} and k_{ti} neglected. Furthermore, it can be noted that when the phospholipid concentration is large, most of the porphyrin molecules are incorporated during the first kinetics phase before flip-flop can occur. Because the porphyrin environment remains lipidic, the redistribution between the two layers does not lead to further fluorescence changes. As a consequence, the amplitude of the second phase is very small. Fluorescence changes recorded upon mixing the porphyrin with vesicles were nicely fitted by monoexponential accordingly. This single phase was analyzed using a simplified expression

$$k^{obs} = k_{on}^{obs}\times[L] + k_{off}^{obs} \quad (5)$$

where k_{on}^{obs} and k_{off}^{obs} are the experimentally observed rate constants for the incorporation of the porphyrin into the

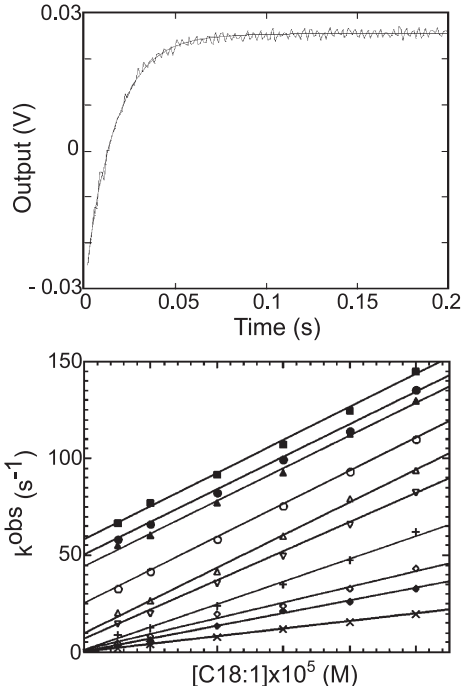

Fig. 6. Stopped-flow study of the kinetics of porphyrin binding to dioleoylphosphatidylcholine (C18:1) unilamellar vesicles. Top: Fluorescence changes following mixing of deuteroporphyrin (10^{-7} M) solutions with vesicles ([C18:1] = 5×10^{-5} M). A monoexponential is shown to perfectly fit the signal. Fits were used to derive pseudo-first order rate constants (see text). Bottom: Linear dependence of the pseudo-first order rate constants on porphyrin concentration at selected pH: (■) 8.5, (●) 8.0, (▲) 7.5, (○) 7.15, (△) 6.6, (▽) 6.3, (+) 5.8, (◇) 5.2, (◆) 5.0, (×) 4.5.

vesicles and for the exit, respectively. The intrinsic rate constants characterizing the various porphyrin forms can be derived from the observed values as shown in the paragraph below. The effect of the pH-dependant ionization state of the porphyrin on these rate constants was investigated using pre-mixing as described above. The aim was first to avoid aging of the solution through precipitation at acidic pH and to limit dimerization. For each pH value, the porphyrin solution was mixed with various concentrations of vesicles. The evolution of the porphyrin fluorescence was fitted by monoexponential and the observed rate constants, k^{obs}, were derived. As shown in Fig. 6, plots of k^{obs} versus the phospholipid concentration were fairly linear in agreement with Eq. (5). The values of k_{on}^{obs} and k_{off}^{obs} were derived from the slope and intercept, respectively. Their dependence on pH is shown in Fig. 7.

3.2.2. Correlation between ionization states of the porphyrin and rate constants of entry and exit from the vesicles

The sigmoid dependence on pH of the curves shown in Fig. 7 indicates that the interaction of the porphyrin with vesicles involves various species with different intrinsic rate constants. However, the monoexponential character of the kinetics indicates that these species cannot be distinguished. This means that equilibrium between these species is reached before entry takes place. Then, the observed rate constants correspond to a combination of those of the various forms of the porphyrin.

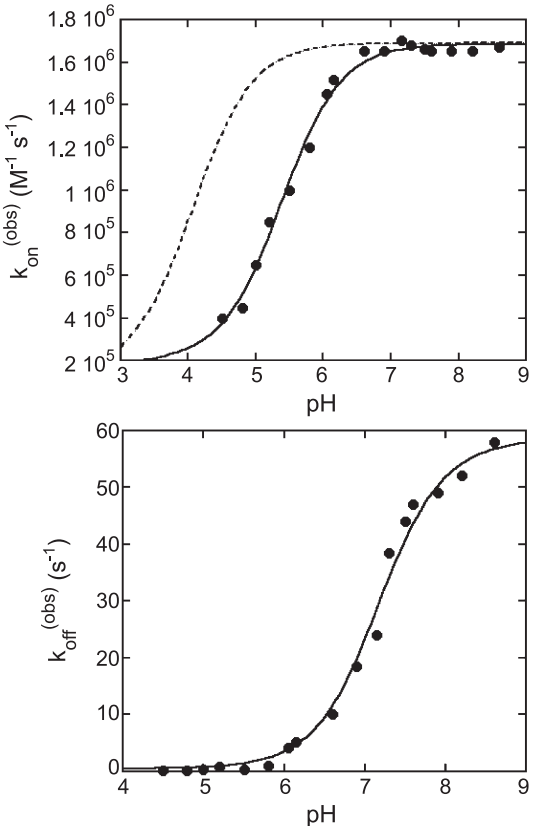

Fig. 7. Effect of pH on the binding of deuteroporphyrin to dioleoylphosphatidylcholine unilamellar vesicles. Top: Association rate constant; the dotted line is the theoretical curve calculated by assuming that protonation of a nitrogen with a pK of 4.1 is responsible for reduction of the rate constant. Bottom: Dissociation rate constant. The parameters used to fit the experimental data are given in the text.

The simplest model corresponds to a single acid–base couple A/B characterized by its pK_a. The observed rate constant would be the sum of the intrinsic rate constant for species A and B weighted by their contribution to the total concentration. The contributions of A and B would be $10^{-pH}/(10^{-pH}+10^{-pK_a})$ and $10^{-pK_a}/(10^{-pH}+10^{-pK_a})$, respectively. The observed rate constant k_{on}^{obs} can be expressed as a function of the intrinsic rate constants k_{on}^{A} and k_{on}^{B}, which yields:

$$k_{on}^{obs} = \frac{k_{on}^{A} + k_{on}^{B} \times 10^{(pH-pK_a)}}{1 + 10^{(pH-pK_a)}} \quad (6)$$

As shown in Fig. 7a, the experimental values of k_{on}^{obs} are conveniently fitted by Eq. 6. In agreement with the observed kinetic effect, the basic form incorporates faster. The best adjustment was obtained with pK_a = 5.39, $k_{on}^{A} = 2.07 \times 10^5$ M^{-1} s^{-1} and $k_{on}^{B} = 1.69 \times 10^6$ M^{-1} s^{-1}. The nature of these species will be discussed later.

The identification of the various forms involved in the exit process is simpler. First, porphyrins are monomeric when incorporated in vesicles. Second, we showed previously that porphyrins protonated at their nitrogens are not incorporated in the phospholipid bilayer [35]. Thus, we have only to consider ionization of the carboxylic chains according to the equilibriums:

$$PH_{2,L} \underset{}{\overset{K_{A1,L}}{\rightleftharpoons}} PH_{,L}^{-} \overset{K_{A2,L}}{\rightleftharpoons} P_{,L}^{2-}$$

where the indice L indicates species incorporated into the bilayer.

The weight of the three species can be calculated as described above, which yields

$$k_{off}^{obs} = \frac{k_{off}^{(2-)} + k_{off}^{(-)} \times 10^{(pK_{A2}-pH)} + k_{off}^{(0)} \times 10^{(pK_{A1}+pK_{A2}-2pH)}}{1 + 10^{(pK_{A2}-pH)} + 10^{(pK_{A1}+pK_{A2}-2pH)}} \quad (7)$$

where $k_{off}^{(2-)}$, $k_{off}^{(-)}$ and $k_{off}^{(0)}$ are the intrinsic rate constants for the exit of P^{2-}, PH^{-} and PH_2, respectively. The best agreement between the experimental points and the theoretical curve was obtained with two close pKs, $pK_{A1,L} = 6.9$ and $pK_{A2,L} = 7.1$ and the following intrinsic rate constants, $k_{off}^{(2-)} = 58.6$ s^{-1}, $k_{off}^{(-)} = 23.5$ s^{-1}, and $k_{off}^{(0)} = 0.46$ s^{-1}.

4. Discussion

In aqueous solution, deuteroporphyrin undergoes self-association processes that are interconnected with complex

acid-base equilibriums. Current knowledge on the behavior of carboxylic porphyrins strongly suggests that dimerization is driven by formation of the neutral form of the porphyrin, PH_2. As a matter of fact, alkaline solutions (pH 8.5–9) of deuteroporphyrin were found to obey Beer's law and spectra showed no evidence for dimer formation up to 3×10^{-6} M. When alkaline solutions are made slightly acidic (pH ~ 5–6), two processes take place in the stopped-flow apparatus. First, acid–base equilibriums are reached. Typical bimolecular rate constants for protonation of carboxylate anions are around 4×10^{10} M^{-1} s^{-1} [36]. For proton concentrations between 10^{-5} and 10^{-6} M (pH 5–6), largely exceeding that of the porphyrin, the pseudo first order rate constant for neutralization of the porphyrin chains will range between about 4×10^{4} to 4×10^{5} s^{-1}. These values correspond to halftimes in the microsecond range, far below the mixing time of our apparatus. Only subsequent processes can be observed.

As shown in Fig. 2b for a pH value of 5.95, the Soret band of the porphyrin is quickly shifted to 370 nm, as compared to the monomer band at 395 nm. In keeping with the exciton theory, this blue shift can be interpreted as the formation of dimers with cofacial stacking [37]. The carboxylic groups on each porphyrin molecule are likely to stand on opposite directions to reduce repulsion [38]. In the range of the concentrations used for absorption measurements, the dimerization process appears to be nearly complete after a few milliseconds as shown in Fig. 2b. Fluorescence detection allowed the use of lower concentrations. This reduced the dimerization rate that became more accessible to stopped-flow measurements. In these conditions, the halftime for dimerization is about 4.2 ms (see Fig. 2e). The signal was well fitted by a single exponential with a rate constant of 164 ± 4 s^{-1}. The monoexponential character of the kinetics suggests that the initial step is the association between a porphyrin with one (or two) carboxylic chain(s) neutralized and any other porphyrin molecules in the bulk solution. The bimolecular rate constant thus derived would be around 3×10^{9} M^{-1} s^{-1}. The limit value for a diffusion-controlled process between two species, A and B, is $k_d = 4\pi R_{AB}(D_A + D_B)N$ where R_{AB} is the encounter distance between the two partners, D_A and D_B their diffusion coefficients and N is the Avogadro number [39]. In the present case, species A and B are both porphyrins. It can be assumed that the encounter distance between the two macrocycles is around 10 Å. The porphyrin diffusion coefficient is about 3.9×10^{-10} m^2 s^{-1} [40]. By using appropriate unit conversion, k_d is calculated to be about 5.9×10^{9} M^{-1} s^{-1}. Taking into account that porphyrins must present appropriate orientation in order to associate, it appears that dimerization is only controlled by diffusion of the porphyrin molecules. Then, the rapidity of dimerization did not allow us to characterize the various ionic states of the monomeric porphyrin by time-resolved spectroscopy and to directly determine pK values.

Alternatively, fluorescence steady-state measurements allowed us to derive the pK values from concentration effect as shown in Fig. 5. The opposite effect on pK_{A1} and pK_{N1} is worth to note. It confirms that the neutral form is involved in dimerization. Indeed, stabilization of the neutral form through self-association at higher concentration disfavors both the ionization of the carboxylic chain and the protonation of the imino nitrogen. An increase of pK_{A1} and a decrease of pK_{N1} values are observed accordingly.

4.1. Porphyrin entry into the phospholipid bilayer

In spite of our precautions, dimers are formed to a significant extent before porphyrins encounter vesicles. Then, the entry of porphyrins into the phospholipid bilayer could depend on both the ionization and the dimerization states of the macrocycle in the bulk aqueous phase. We can have some insight into the entry process by considering the state of the porphyrin after incorporation. First, within the range of phospholipid/porphyrin ratio investigated, the porphyrin exists as monomer in vesicles. Spectroscopic and kinetic data indicate that the porphyrin lies with its core embedded into the lipid phase of the vesicles and its carboxylic chains, ionized or not, oriented towards the aqueous interface [26,41]. Second, whatever the pH, incorporated porphyrins are not protonated on nitrogens [35]. Dimers of porphyrins with asymmetrical distribution of ionic side chains such as deuteroporphyrin are generally characterized by cofacial stacking, the polar groups standing on opposite directions to reduce repulsion. The distribution of polar chains in the dimer is roughly symmetrical, which is not favorable for incorporation. All these considerations indicate that both protonation of inner nitrogens and dimerization would decrease the rate of incorporation in the vesicles.

Experimentally, we found that the rate constant for entry is lowered with decreasing pH. The data were well fitted assuming a simple acid–base equilibrium with a pK of 5.39. Because protonation and dimerization equilibriums are interconnected, the assignment of species responsible for the observed effect is not straightforward. As shown in Fig. 7 (dotted line in top panel), the nitrogen protonation would lead to an effect rather different from that observed if a pK_{N1} value of 4.1 is assumed. However, the local pH near the lipidic interface may be different from that of the aqueous solution [43]. In addition, in the range of pH corresponding to the experimentally determined pK value, porphyrins show a strong tendency to form dimers. As outlined above, dimerization is driven by the neutral species, PH_2 that is formed through neutralization of the monoanionic form. The corresponding pK, pK_{A1} is 5.3 for infinite dilution. This value is shifted to 5.5 at the concentrations used in the stopped flow experiments (see Fig. 5). Then, a decrease of the entry rate due to dimerization of the porphyrins in the bulk aqueous phase appears also very likely.

4.2. Exit from the vesicles

The two carboxylic chains of the porphyrin at the lipidic interface were characterized by close pK values at 6.9 and 7.3, respectively (see Fig. 7). In keeping with previous observations, a significant shift of pK is observed when the porphyrin is incorporated within the vesicles [42]. Although the errors on the values of $k_{\mathrm{off}}^{(2-)}$, $k_{\mathrm{off}}^{(-)}$ and $k_{\mathrm{off}}^{(0)}$ are important owing to the multiparametric nature of the fit, it is clear that the dianionic form of the porphyrin leaves the bilayer more easily than the more hydrophobic forms. These results corroborate previous data obtained by a methodology based on the transfer of porphyrins from vesicles to albumin [27,28].

4.3. A dynamic model for the traffic of dicarboxylic porphyrins through biological membranes

The present results emphasize the importance of pH in the control of the entry of dicarboxylic porphyrins into membranes. In addition to our previous studies, they bring a dynamic vision of the cellular traffic of these molecules. The entry of porphyrins into the external layer of membranes is very fast until the pH value is lowered below 6.5. Besides, the transfer of the porphyrin through the bilayer is greatly accelerated when the pH is decreased from 7.5 to 6.5. In the same pH range, but in an opposite way, the exit of the porphyrin from the other side of the membrane is strongly facilitated [27,28]. Then, all the present data support the hypothesis that pH effects contribute to the selectivity of carboxylic photosensitizers for tumors significantly. The acidification of the tumor interstitial liquid down to a typical value of 6.9 while the intracellular pH of cancer cells remains to a normal value around 7.4 provides a pH gradient favoring photosensitizer uptake. In must be pointed out that this small range of pH values corresponds to an optimal zone of effectiveness if we consider the rate constants for the entry, transfer and exit in the cytoplasmic compartment. This mechanism is likely to apply to other amphiphilic photosensitizers bearing carboxylic chains as exemplified by Photofrin® [23] and chlorin e6 [44].

Incorporation of carboxylic photosensitizers by bulk or receptor-mediated endocytosis might lead to a more complex situation. Indeed, in the course of its traffic in the endosome/lysosome compartment, the porphyrin would encounter pH values from the neutrality to values as low as 5. In the most acidic compartments, the porphyrin may self-associate reducing the overall rate of entry into the bilayer. This step could be rate-limiting although the transfer through the membrane would be favored in this pH range. This effect would be reinforced by the high local concentration of porphyrin that results from the small size of the endosomes or lysosomes. The porphyrin would escape more easily from the early less acidic endosomes.

5. Conclusion

By fulfilling the studies on the aqueous properties and the interactions of dicarboxylic porphyrins with phospholipidic bilayers in a large range of pH, we are now able to describe all the steps involved in the passive transport of these molecules through membranes. This transport is highly dependent on pH that influences the dynamics of all the elementary steps, i.e. the entry, the flip-flop between the two layers and the exit from the membrane. As a whole, these results consolidate the idea of a selectivity of amphiphilic carboxylic molecules for tumor based on pH effects. They also show that intracellular traffic is also governed by pH but in a more complex way that may involve pH-dependent self-association of the photosensitizer.

Acknowledgements

The authors thank Dr. C. Vever-Bizet for her kind support during this work. The stopped-flow apparatus was acquired, thanks to subsidy from ARC (grant #7209).

References

[1] J.D. Spikes, Photodynamic reactions in photomedicine, in: J.D. Regan, J.A. Parrish (Eds.), The Science of Photomedicine, Plenum, New York, 1982, pp. 113–144.
[2] R.L. Lipson, E.J. Baldes, A.M. Olsen, The use of a derivative of hematoporphyrin in tumor detection, J. Natl. Cancer Inst. 26 (1961) 1–11.
[3] T.J. Dougherty, W.R. Potter, D. Bellnier, Photodynamic therapy for treatment of cancer: current status and advances, in: D. Kessel (Ed.), Photodynamic Therapy of Neoplastic Disease, CRC Press, Boston, USA, 1990, pp. 1–19.
[4] T.J. Dougherty, C.J. Gomer, B.W. Henderson, G. Jori, D. Kessel, M. Korbelik, J. Moan, Q. Peng, Photodynamic therapy, J. Natl. Cancer Inst. 90 (1998) 889–905.
[5] U. Schmidt-Erfurth, T. Hasan, K. Schomacker, T. Flotte, R. Birngruber, In vivo uptake of liposomal benzoporphyrin derivative and photothrombosis in experimental corneal neovascularization, Lasers Surg. Med. 17 (1995) 178–188.
[6] U. Schmidt-Erfurth, T.J. Flotte, E.S. Gragoudas, K. Schomacker, R. Birngruber, T. Hasan, Benzoporphyrin-lipoprotein-mediated photodestruction of intraocular tumors, Exp. Eye Res. 62 (1996) 1–10.
[7] K.W. Woodburn, N.J. Vardaxis, J.S. Hill, A.H. Kaye, J.A. Reiss, D.R. Phillips, Evaluation of porphyrin characteristics required for photodynamic therapy, Photochem. Photobiol. 55 (1992) 697–704.
[8] M. Dellinger, Apoptosis or necrosis following Photofrin photosensitization: influence of the incubation protocol, Photochem. Photobiol. 64 (1996) 182–187.
[9] D. Kessel, Y. Luo, Y. Deng, C.K. Chang, The role of subcellular localization in initiation of apoptosis by photodynamic therapy, Photochem. Photobiol. 65 (1997) 422–426.
[10] M. Beltramini, P.A. Firey, F. Ricchelli, M.A. Rodgers, G. Jori, Steady-state and time-resolved spectroscopic studies on the hematoporphyrin-lipoprotein complex, Biochemistry 26 (1987) 6852–6858.
[11] G. Jori, M. Beltramini, E. Reddi, B. Salvato, A. Pagnan, L. Ziron, L. Tomio, T. Tsanov, Evidence for a major role of plasma lipoproteins as hematoporphyrin carriers in vivo, Cancer Lett. 24 (1984) 291–297.
[12] D. Kessel, Porphyrin-lipoprotein association as a factor in porphyrin localization, Cancer Lett. 33 (1986) 183–188.

[13] J.C. Maziere, P. Morliere, R. Santus, The role of the low density lipoprotein receptor pathway in the delivery of lipophilic photosensitizers in the photodynamic therapy of tumours, J. Photochem. Photobiol., B Biol. 8 (1991) 351–360.
[14] D. Gal, P.C. MacDonald, J.C. Porter, E.R. Simpson, Cholesterol metabolism in cancer cells in monolayer culture. III. Low-density lipoprotein metabolism, Int. J. Cancer 28 (1981) 315–319.
[15] S. Vitols, C. Peterson, O. Larsson, P. Holm, B. Aberg, Elevated uptake of low density lipoproteins by human lung cancer tissue in vivo, Cancer Res. 52 (1992) 6244–6247.
[16] S. Bonneau, C. Vever-Bizet, P. Morliere, J.C. Maziere, D. Brault, Equilibrium and kinetic studies of the interactions of a porphyrin with low-density lipoproteins, Biophys. J. 83 (2002) 3470–3481.
[17] W.D. Stein, Transport and Diffusion Across Cell Membranes, Academic Press, New York, 1986.
[18] M. Kepczynski, R.P. Pandian, K.M. Smith, B. Ehrenberg, Do liposome-binding constants of porphyrins correlate with their measured and predicted partitioning between octanol and water? Photochem. Photobiol. 76 (2002) 127–134.
[19] I.F. Tannock, D. Rotin, Acid pH in tumors and its potential for therapeutic exploitation, Cancer Res. 49 (1989) 4373–4384.
[20] D. Brault, C. Vever-Bizet, T. Le Doan, Spectrofluorimetric study of porphyrin incorporation into membrane models - evidence for pH effects, Biochim. Biophys. Acta 857 (1986) 238–250.
[21] R. Pottier, J.C. Kennedy, The possible role of ionic species in selective biodistribution of photochemotherapeutic agents toward neoplastic tissue, J. Photochem. Photobiol., B Biol. 8 (1990) 1–16.
[22] A.J. Barrett, J.C. Kennedy, R.A. Jones, P. Nadeau, R.H. Pottier, The effect of tissue and cellular pH on the selective biodistribution of porphyrin-type photochemotherapeutic agents: a volumetric titration study, J. Photochem. Photobiol., B Biol. 6 (1990) 309–323.
[23] J.P. Thomas, A.W. Girotti, Glucose administration augments in vivo uptake and phototoxicity of the tumor-localizing fraction of hematoporphyrin derivative, Photochem. Photobiol. 49 (1989) 241–247.
[24] J. Moan, L. Smedshammer, T. Christensen, Photodynamic effects on human cells exposed to light in the presence of hematoporphyrin. pH effects, Cancer Lett. 9 (1980) 327–332.
[25] M. Kepczynski, B. Ehrenberg, Interaction of dicarboxylic metalloporphyrins with liposomes. The effect of pH on membrane binding revisited, Photochem. Photobiol. 76 (2002) 486–492.
[26] K. Kuzelova, D. Brault, Kinetic and equilibrium studies of porphyrin interactions with unilamellar lipidic vesicles, Biochemistry 33 (1994) 9447–9459.
[27] K. Kuzelova, D. Brault, Interactions of dicarboxylic porphyrins with unilamellar lipidic vesicles: drastic effects of pH and cholesterol on kinetics, Biochemistry 34 (1995) 11245–11255.
[28] N. Maman, D. Brault, Kinetics of the interactions of a dicarboxylic porphyrin with unilamellar lipidic vesicles: interplay between bilayer thickness and pH in rate control, Biochim. Biophys. Acta 1414 (1998) 31–42.
[29] W.I. White, Aggregation of porphyrins and metalloporphyrins, in: D. Dolphin (Ed.), The Porphyrins, Academic Press, New York, 1978, pp. 303–339.
[30] S.B. Brown, M. Shillcock, P. Jones, Equilibrium and kinetic studies of the aggregation of porphyrins in aqueous solution, Biochem. J. 153 (1976) 279–285.
[31] R. Margalit, M. Rotenberg, Thermodynamics of porphyrin dimerization in aqueous solutions, Biochem. J. 219 (1984) 445–450.
[32] K.M. Smith, Porphyrins and Metalloporphyrins, Elsevier, Amsterdam, 1975.
[33] J.R. Lakowicz, Principles of Fluorescence Spectroscopy, Plenum, New York, 1983.
[34] H. Morales-Rojas, A.K. Yatsimirsky, Medium effects on the dimerization of coproporphyrin-I free base, J. Phys. Org. Chem. 12 (1999) 377–387.
[35] D. Brault, C. Vever-Bizet, K. Kuzelova, Interactions of dicarboxylic porphyrins with membranes in relation to their ionization state, J. Photochem. Photobiol., B Biol. 20 (1993) 191–195.
[36] M. Eigen, W. Kruse, G. Maass, L. De Maeyer, Rate constants of protolytic reactions in aqueous solution, in: G. Porter (Ed.), Progress in Reaction Kinetics, Pergamon, Oxford, 1964, pp. 287–318.
[37] M. Kasha, Energy transfer mechanisms and the molecular exciton model for molecular aggregates, Radiat. Res. 20 (1963) 55–70.
[38] J. Dairou, C. Vever-Bizet, D. Brault, Self-association of disulfonated deuteroporphyrin and its esters in aqueous solution and photosensitized production of singlet oxygen by the dimers, Photochem. Photobiol. 75 (2002) 229–236.
[39] P.W. Atkins, Physical Chemistry, 4th ed., Oxford Univ. Press, Oxford, 1990.
[40] C. Vever-Bizet, D. Brault, Kinetics of incorporation of porphyrins into small unilamellar vesicles, Biochim. Biophys. Acta 1153 (1993) 170–174.
[41] A. Lavi, H. Weitman, R.T. Holmes, K.M. Smith, B. Ehrenberg, The depth of porphyrin in a membrane and the membrane's physical properties affect the photosensitizing efficiency, Biophys. J. 82 (2002) 2101–2110.
[42] M. Egret-Charlier, A. Sanson, M. Ptak, Ionization of fatty acids at the lipid–water interface, FEBS Lett. 89 (1978) 313–316.
[43] D.A. Cherepanov, B.A. Feniouk, W. Junge, A.Y. Mulkidjanian, Low dielectric permittivity of water at the membrane interface: effect on the energy coupling mechanism in biological membranes, Biophys. J. 85 (2003) 1307–1316.
[44] B. Cunderlikova, L. Gangeskar, J. Moan, Acid-base properties of chlorin e6: relation to cellular uptake, J. Photochem. Photobiol., B Biol. 53 (1999) 81–90.